

# Differential Expression of Sodium Channel $\beta$ Subunits in Dorsal Root Ganglion Sensory Neurons\*

Received for publication, December 14, 2011, and in revised form, March 6, 2012. Published, JBC Papers in Press, March 9, 2012, DOI 10.1074/jbc.M111.333740

Cojen Ho<sup>‡</sup>, Juan Zhao<sup>§</sup>, Steven Malinowski<sup>‡</sup>, Mohamed Chahine<sup>§</sup>, and Michael E. O'Leary<sup>‡1</sup>

From the <sup>‡</sup>Department of Pathology, Anatomy, and Cell Biology, Thomas Jefferson University, Philadelphia, Pennsylvania 19107 and the <sup>§</sup>Centre de Recherche Université Laval Robert-Giffard, Université Laval, Québec G1J 2G3, Canada

**Background:** Auxiliary  $\beta$  subunits regulate the voltage-gated sodium channels of dorsal root ganglion (DRG) neurons.

**Results:**  $\beta$  subunits are differentially expressed in subpopulations of DRG neurons and regulate Na<sub>v</sub>1.7 channels in an isoform-specific manner.

**Conclusion:** Differential  $\beta$  subunit expression and isoform-specific regulation have important implications for the sodium currents of DRG neurons.

**Significance:**  $\beta$  subunits are important determinants of sodium channel function and sensory neuron excitability.

The small-diameter (<25  $\mu\text{m}$ ) and large-diameter (>30  $\mu\text{m}$ ) sensory neurons of the dorsal root ganglion (DRG) express distinct combinations of tetrodotoxin sensitive and tetrodotoxin-resistant Na<sup>+</sup> channels that underlie the unique electrical properties of these neurons. *In vivo*, these Na<sup>+</sup> channels are formed as complexes of pore-forming  $\alpha$  and auxiliary  $\beta$  subunits. The goal of this study was to investigate the expression of  $\beta$  subunits in DRG sensory neurons. Quantitative single-cell RT-PCR revealed that  $\beta$  subunit mRNA is differentially expressed in small ( $\beta_2$  and  $\beta_3$ ) and large ( $\beta_1$  and  $\beta_2$ ) DRG neurons. This raises the possibility that  $\beta$  subunit availability and Na<sup>+</sup> channel composition and functional regulation may differ in these subpopulations of sensory neurons. To further explore these possibilities, we quantitatively compared the mRNA expression of the  $\beta$  subunit with that of Na<sub>v</sub>1.7, a TTX-sensitive Na<sup>+</sup> channel widely expressed in both small and large DRG neurons. Na<sub>v</sub>1.7 and  $\beta$  subunit mRNAs were significantly correlated in small ( $\beta_2$  and  $\beta_3$ ) and large ( $\beta_1$  and  $\beta_2$ ) DRG neurons, indicating that these subunits are coexpressed in the same populations. Co-immunoprecipitation and immunocytochemistry indicated that Na<sub>v</sub>1.7 formed stable complexes with the  $\beta_1$ – $\beta_3$  subunits *in vivo* and that Na<sub>v</sub>1.7 and  $\beta_3$  co-localized within the plasma membranes of small DRG neurons. Heterologous expression studies showed that  $\beta_3$  induced a hyperpolarizing shift in Na<sub>v</sub>1.7 activation, whereas  $\beta_1$  produced a depolarizing shift in inactivation and faster recovery. The data indicate that  $\beta_3$  and  $\beta_1$  subunits are preferentially expressed in small and large DRG neurons, respectively, and that these auxiliary subunits differentially regulate the gating properties of Na<sub>v</sub>1.7 channels.

The sensory neurons of the dorsal root ganglia (DRG)<sup>2</sup> give rise to nerve fibers that convey information about thermal, mechanical, and chemical stimulation from peripheral tissues to the central nervous system. These neurons express a unique combination of tetrodotoxin-sensitive (TTX-S) and tetrodotoxin-resistant (TTX-R) Na<sup>+</sup> currents that produce the rapid rising phase of the action potentials. Much of what is currently known about Na<sup>+</sup> channel expression in sensory neurons has been derived from electrophysiological studies of cultured DRG neurons (1–3). The small-diameter neurons (<25  $\mu\text{m}$ ) isolated from the DRG represent the cell bodies of unmyelinated nociceptors and preferentially express TTX-R Na<sup>+</sup> current, whereas the large-diameter neurons (>30  $\mu\text{m}$ ), typically associated with low threshold mechanoreceptors, predominantly express TTX-S Na<sup>+</sup> current. DRG sensory neurons express at least six distinct Na<sup>+</sup> channel isoforms that display properties similar to the endogenous TTX-S (Na<sub>v</sub>1.1, Na<sub>v</sub>1.2, Na<sub>v</sub>1.6, and Na<sub>v</sub>1.7) and TTX-R (Na<sub>v</sub>1.8 and Na<sub>v</sub>1.9) Na<sup>+</sup> currents observed in these neurons (4–7).

*In vivo*, voltage-gated sodium channels form complexes with auxiliary  $\beta$  subunits that regulate the trafficking, gating properties, and kinetics of the endogenous Na<sup>+</sup> channels (8–12).  $\beta$  subunits are relatively small proteins (33–36 kDa) composed of a single membrane-spanning  $\alpha$  helix, a short intracellular C terminus, and a large extracellular N terminus incorporating an immunoglobulin-like fold similar to that found in adhesion molecules (8, 13). Immunocytochemistry and *in situ* hybridization indicate that all four isoforms of the  $\beta$  subunit ( $\beta_1$ – $\beta_4$ ) are expressed in sensory neurons (12, 14, 15).

In this study, we employed a combination of single-cell RT-PCR, immunocytochemistry, immunoprecipitation, and electrophysiology to further investigate  $\beta$  subunit expression in DRG sensory neurons. The data indicate that small and large DRG neurons express different complements of  $\beta$  subunits. The functional consequences of  $\beta$  subunit expression were evaluated by examining their regulation of Na<sub>v</sub>1.7, a TTX-S Na<sup>+</sup> channel widely expressed in sensory neurons and an

\* This work was supported, in whole or in part, by National Institutes of Health Grant R01 GM078244 from NIGMS (to M. E. O'L.). This work was also supported by the Heart and Stroke Foundation of Québec (HSFQ) and Canadian Institutes of Health Research (CIHR) Grant INO-77909 (to M. C.).

<sup>1</sup> To whom correspondence should be addressed: Dept. of Pathology, Anatomy, and Cell Biology, Thomas Jefferson University, 1020 Locust St., JAH 473, Philadelphia, PA 19107. Tel.: 215-503-9983; E-mail: michael.oleary@jefferson.edu.

<sup>2</sup> The abbreviations used are: DRG, dorsal root ganglion/ganglia; TTX-S, tetrodotoxin-sensitive; TTX-R, tetrodotoxin-resistant.

important contributor to pain sensation (19, 20). The  $\beta_3$  and  $\beta_1$  subunits differentially regulated heterologously expressed  $\text{Na}_v1.7$  channels. The preferential expression of  $\beta$  subunits in small ( $\beta_2$  and  $\beta_3$ ) and large ( $\beta_1$  and  $\beta_2$ ) neurons, coupled with the isoform-specific  $\beta$  subunit regulation of  $\text{Na}_v1.7$  activation ( $\beta_3$ ) and inactivation ( $\beta_1$ ), predicts substantial differences in the TTX-S currents of DRG sensory neurons.

## EXPERIMENTAL PROCEDURES

**Preparation of DRG Neurons**—Postnatal day 7 Sprague-Dawley rats (P7) were anesthetized with isoflurane before decapitation, and the DRG were harvested from all accessible levels. The ganglia were incubated for 30 min at 37 °C in 2 ml of Hanks' balanced salt solution/HEPES containing 1.5 mg/ml collagenase (Sigma-Aldrich), followed by 1 mg/ml trypsin (Sigma-Aldrich) for an additional 30 min. Trypsin was removed, and the ganglia were transferred to Leibovitz's L-15 medium supplemented with 1% fetal bovine serum (Invitrogen), 2 mM glutamine, 2% penicillin/streptomycin (Invitrogen), and 50 ng/ml nerve growth factor (Sigma-Aldrich). The ganglia were disrupted using fire-polished Pasteur pipettes, and dissociated neurons were plated onto polylysine-coated glass coverslips and placed into 35-mm dishes containing supplemented Leibovitz's medium. Neurons were suitable for single-cell harvesting and electrophysiology for up to 8 h after plating. Animal protocols were approved by the Animal Care and Use Committee of Thomas Jefferson University.

**Single-cell RT-PCR**—Detailed methods for performing single-cell RT-PCR with dissociated DRG neurons were published recently (7). Small-diameter (<25  $\mu\text{m}$ ) and large-diameter (>30  $\mu\text{m}$ ) DRG neurons were individually harvested by drawing them into a large bore pipette (30–50- $\mu\text{m}$  diameter) containing sterile bath solution. The neurons were osmotically lysed by 10-fold dilution with sterile water and rapidly frozen. The mRNA present in the cell lysates was reverse-transcribed using random hexamer primers (Stratagene) in a standard 25- $\mu\text{l}$  Moloney murine leukemia virus reverse transcription reaction (Fisher). Aliquots of the transcription reaction (1–2  $\mu\text{l}$ ) were quantitatively analyzed using a SYBR Green reaction mixture on an Mx30005P real-time PCR machine (Agilent Technologies).  $\beta$ -Actin was quantitatively measured in each sample and used to normalize for differences in cellular mRNA expression. The absolute number of mRNA copies of each transcript was determined by comparing the threshold cycle ( $C_t$ ) of the single-cell lysates with known cDNA standards assayed in parallel reactions. PCR primers were designed to span exon/intron borders to eliminate the detection of genomic DNA, and concentrations (50–200 nM) were optimized to achieve high amplification efficiency without the formation of primer dimers (Prologo, Sigma-Aldrich). The specificity of the real-time detections was assessed using melting curve analysis, and the identity of the amplified DNA was determined by sequencing.

**$\text{Na}_v1.7$  Stable Cell Line**—Rat  $\text{Na}_v1.7$  cDNA was subcloned into the pcDNA3 expression vector (Invitrogen) and transfected into HEK293 cells using a standard calcium phosphate precipitation method (Invitrogen). After 2 weeks of selection for neomycin resistance (800  $\mu\text{g/ml}$ ), the remaining colonies

were isolated and transferred to separate culture plates for expansion.  $\text{Na}_v1.7$  expression was verified using RT-PCR and electrophysiology to measure  $\text{Na}^+$  currents. The HEK293 cell line stably expressing  $\text{Na}_v1.7$  was maintained under standard culture conditions in DMEM supplemented with 10% FBS, 2 mM L-glutamine, 100 units/ml penicillin, 10 mg/ml streptomycin, and 400  $\mu\text{g/ml}$  neomycin (Invitrogen).

**Electrophysiology**—Macroscopic  $\text{Na}^+$  currents of HEK293 cells stably expressing the  $\text{Na}_v1.7$  channel were recorded using the whole-cell patch clamp technique. The pipette solution contained 5 mM NaCl, 135 mM CsF, 10 mM EGTA, and 10 mM HEPES (pH 7.4). The bath solution contained 150 mM NaCl, 2 mM KCl, 1.5 mM  $\text{CaCl}_2$ , 1 mM  $\text{MgCl}_2$ , and 10 mM HEPES (pH 7.4). Patch electrodes were fashioned from Corning 8161 borosilicate glass and coated with Sylgard (Dow Corning Corp.) to minimize pipette capacitance. Recording pipettes had low access resistances (<1 megohm), and the residual series resistance was 80% compensated. A correction for the liquid junction potential between the pipette and the bath solutions (–7 mV) was applied to the holding potential before the formation of gigohm seals. After establishing the whole-cell configuration, the cells were dialyzed for 10 min at room temperature (22 °C) prior to recording  $\text{Na}^+$  currents. Voltage pulses were generated, and currents were recorded using pCLAMP and an Axopatch 200 amplifier (Molecular Devices). Whole-cell currents were filtered at 5 kHz and digitized at 10 kHz with a Digidata 1440A system (Molecular Devices).

Current-voltage relationships were obtained by plotting the current density (picoamperes/picofarad) versus the test voltage. Normalized  $\text{Na}^+$  conductance ( $G_{\text{Na}}$ ) was calculated from the peak  $\text{Na}^+$  current ( $I_{\text{Na}}$ ) at each test potential ( $V$ ):  $G_{\text{Na}} = I_{\text{Na}} / (V - E_{\text{Na}})$ , where  $E_{\text{Na}}$  is the measured  $\text{Na}^+$  ion reversal potential. The steady-state inactivation was determined by normalizing the peak  $\text{Na}^+$  current ( $I$ ) measured after conditioning prepulses (–130 to –10 mV for 500 ms) to the maximal  $\text{Na}^+$  current amplitude ( $I_{\text{max}}$ ) measured after prepulses to –140 mV and plotted against the conditioning voltage. The activation and steady-state inactivation were fitted to Boltzmann functions:  $G/G_{\text{max}}(I/I_{\text{max}}) = 1 / (1 + \exp((V_{0.5} - V)/k_v))$ , where  $V_{0.5}$  is the midpoint, and  $k_v$  is the slope factor. The predicted window currents were calculated from the product of the activation and steady-state inactivation curves as described previously (21). Recovery from inactivation was determined using depolarizing prepulses (–30 mV/20 ms) before returning to –100 mV for variable intervals (0–1200 ms). Standard test pulses (–30 mV/20 ms) were used to assess availability. The recovery time course was fitted to the sum of two exponentials, yielding estimates of the fast ( $\tau_f$ ) and slow ( $\tau_s$ ) time constants.

Rat  $\beta_1$ – $\beta_3$  subunits were cloned in our laboratory as described previously (22). The  $\beta_4$  subunit was a gift from Dr. Lori Isom (University of Michigan). The  $\text{Na}^+$  channel  $\beta_1$ – $\beta_4$  subunits (piRES/CD8/ $\beta_{1-4}$ ) and CD8 cDNA were subcloned into the piRES vector (Clontech). HEK293 cells stably expressing the  $\text{Na}_v1.7$  channel were transiently transfected with piRES/CD8/ $\beta_{1-4}$  cDNA using a calcium phosphate precipitation method (23). Prior to recording, the cells were briefly incubated in PBS containing anti-CD8 antibody-coated beads to identify cells expressing the CD8 antigen (Dynal, Lake Success, NY).

## Differential Expression of $\beta$ Subunits in DRG Neurons

**$\beta$  Subunit Chimeras**—The  $\beta_1/\beta_2$  chimeras ( $\beta_{211}$ ,  $\beta_{221}$ ,  $\beta_{112}$ , and  $\beta_{11\Delta}$ ) were a gift from Dr. Thomas Zimmer (Friedrich-Schiller Universität, Jena, Germany). The three subscripted numbers refer to the extracellular N-terminal, membrane-spanning, and intracellular C-terminal domains. In this nomenclature, the wild-type  $\beta_1$  and  $\beta_2$  subunits are designated  $\beta_{111}$  and  $\beta_{222}$ , respectively.  $\beta_{211}$  contains the extracellular domain of  $\beta_2$  and the membrane-spanning and intracellular domains of  $\beta_1$ .  $\beta_{221}$  incorporates the extracellular and membrane-spanning domains of  $\beta_2$  and the intracellular domain of  $\beta_1$ .  $\beta_{112}$  contains the extracellular and membrane-spanning domains of  $\beta_1$  and the intracellular domain of  $\beta_2$ .  $\beta_{11\Delta}$  contains the extracellular and membrane-spanning domains of  $\beta_1$  and a deletion of the 41 amino acids from the intracellular C-terminal domain (see Fig. 6A).  $\beta_{211}$ ,  $\beta_{221}$ ,  $\beta_{112}$ , and  $\beta_{11\Delta}$  were transferred to the piRES vector for expression in mammalian cells (piRES/CD8/ $\beta_{211}$ , piRES/CD8/ $\beta_{221}$ , piRES/CD8/ $\beta_{112}$ , and piRES/CD8/ $\beta_{11\Delta}$ ) and transiently transfected into our  $\text{Na}_v1.7$  stable cell line.

**Immunoprecipitation and Western Analysis**—Rat DRG were harvested and immediately placed in ice-cold Hanks' balanced salt solution. The ganglia were washed with ice-cold Hanks' balanced salt solution and pelleted by low speed centrifugation at 4 °C. Hanks' balanced salt solution was replaced with ice-cold lysis buffer (50 mM Tris, 1.0 mM EDTA, 1.0 mM EGTA, 150 mM NaCl, and 1.0% Triton X-100) supplemented with protease inhibitors (Sigma-Aldrich). The samples were homogenized on ice and centrifuged at 15,000 rpm for 20 min at 4 °C. The supernatant was recovered and assayed for protein concentration using the Bradford method (Bio-Rad). Lysates (1 mg) were incubated overnight at 4 °C in 1 ml of lysis buffer containing either 10  $\mu\text{g}$  of control mouse IgG or 10  $\mu\text{g}$  of mouse anti- $\text{Na}_v1.7$  monoclonal antibody N68/6 (UC Davis/NIH NeuroMab Facility). Anti- $\text{Na}_v1.7$  antibody N68/6 does not cross-react with other  $\text{Na}^+$  channel isoforms or channel proteins extracted from adult rat brain. Protein G-agarose resin (Thermo Scientific) was added (100  $\mu\text{l}$ ), and the lysates were incubated for 6 h at 4 °C before washing with ice-cold lysis buffer. Proteins were eluted from the protein G-agarose by the addition of 50  $\mu\text{l}$  of 0.2 M glycine buffer (pH 2.5). The pH was neutralized by adding 10  $\mu\text{l}$  of 1 M Tris buffer (pH 9.0), mixed with 3 $\times$  sample buffer, and separated on 12% SDS-polyacrylamide gels. Proteins were transferred to Protran nitrocellulose membranes (Whatman); blocked with 5% BSA; washed with Tris-buffered saline with 0.1% Tween 20 (TBS/Tween); and incubated overnight with rabbit anti-SCN1B (Cell Applications), rabbit anti-SCN2B (Sigma-Aldrich), or rabbit anti-SCN3B (Abcam) polyclonal antibody in TBS/Tween containing 5% BSA. These commercial antibodies (SCN1B, SCN2B, and SCN3B) are highly specific and do not display cross-reactivity with other members of the  $\beta$  subunit family. The membranes were incubated with HRP-conjugated goat anti-rabbit secondary antibody (Thermo Scientific) for 1 h at room temperature, and labeled proteins were detected by chemiluminescence (Thermo Scientific). We routinely failed to observe  $\text{Na}_v1.7$  or  $\beta$  subunit precipitation from cell lysates preincubated with control IgG, further supporting the specificity of the  $\text{Na}_v1.7$  immunoprecipitations. The low level expression of the  $\beta_4$  subunits in DRG neurons (see Fig. 1)

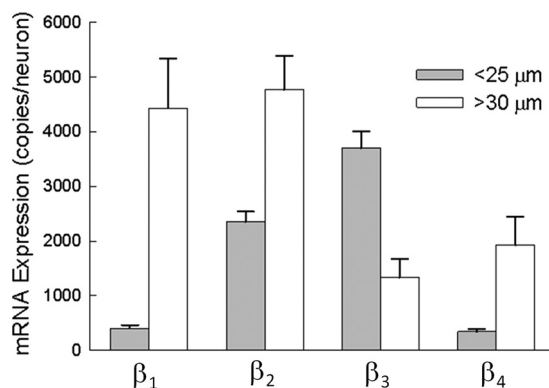


**FIGURE 1. Single-cell analysis of  $\beta$  subunit mRNA.** Small-diameter (<25  $\mu\text{m}$ ) and large-diameter (>30  $\mu\text{m}$ ) DRG neurons were individually harvested, and the mRNA present in the cell lysates was reverse-transcribed and quantitatively measured by real-time PCR. The data are expressed as the number of mRNA copies present in each neuron. The data are the means  $\pm$  S.E. of 74 small and 21 large neurons.

combined with the poor quality of available anti- $\beta_4$  antibodies prevented detailed analysis of this protein.

**Immunocytochemistry**—Dissociated DRG neurons were plated onto polylysine-coated glass coverslips and fixed in PBS containing 4% paraformaldehyde for 10 min. Cells were permeabilized with 0.1% Triton X-100 in PBS for 5 min before several washes with PBS. Nonspecific antibody binding was reduced by incubating the cells with 5% BSA and 5% goat serum in TBS/Tween for 60 min. Permeabilized cells were incubated with mouse anti- $\text{Na}_v1.7$  monoclonal antibody or rabbit anti-SCN1B, rabbit anti-SCN2B, or rabbit anti-SCN3B polyclonal antibody (1:500 dilution) for 60 min before adding Alexa Fluor 488-conjugated anti-mouse or Alexa Fluor 594-conjugated anti-rabbit fluorescent secondary antibody (Invitrogen) for 60 min. After several washes with PBS, the coverslips were dried overnight and mounted onto glass slides with Mowiol 4.88 (Calbiochem). The slides were imaged on a Zeiss LSM 510 META confocal microscope equipped with FITC and rhodamine filter sets at the Kimmel Cancer Center at Jefferson Medical College.

## RESULTS

The expression of  $\beta$  subunits was investigated in acutely dissociated DRG sensory neurons isolated from 7-day-old neonatal rats. Neurons were individually harvested, and the mRNA present in the cell lysates was quantitatively measured (mRNA copies/neuron) using real-time PCR. Fig. 1 compares the expression of the  $\beta$  subunit transcripts in small-diameter (<25  $\mu\text{m}$ ) and large-diameter (>30  $\mu\text{m}$ ) DRG neurons. The data indicate that small neurons preferentially expressed the  $\beta_2$  and  $\beta_3$  isoforms (2000–4000 copies/neuron). Although  $\beta_1$  was also detected in these neurons, the mRNA copy number was 5-fold lower (<400 copies/neuron). This contrasts with large-diameter neurons, which highly expressed  $\beta_1$  and  $\beta_2$  mRNAs ( $\approx$ 4500 copies/neuron), whereas  $\beta_3$  was present at lower levels (<2000 copies/neuron). The  $\beta_4$  subunit was expressed at comparatively low levels in both the small (<500 copies/neuron) and large (<2000 copies/neuron) neurons. The data indicate that small ( $\beta_2$  and  $\beta_3$ ) and large ( $\beta_1$  and  $\beta_2$ ) DRG neurons express different complements of auxiliary  $\beta$  subunits.



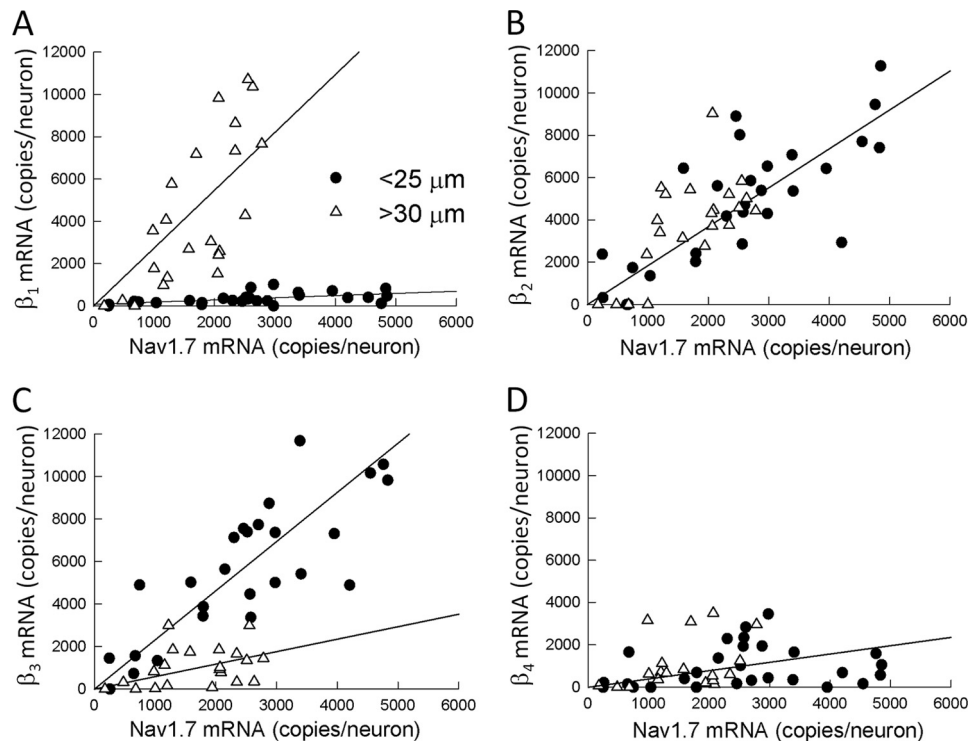


**FIGURE 2. Correlation of  $\text{Na}_v1.7$  and  $\beta$  subunit mRNA expression in small and large DRG neurons.** The mRNAs (copies/neuron) of  $\text{Na}_v1.7$  and  $\beta$  subunits were measured in the same populations of small-diameter ( $<25 \mu\text{m}$ ) and large-diameter ( $>30 \mu\text{m}$ ) neurons. Plots are shown of  $\text{Na}_v1.7$  mRNA versus  $\beta_1$  (A),  $\beta_2$  (B),  $\beta_3$  (C), and  $\beta_4$  (D). The straight lines are simple linear regressions. The data represent the means  $\pm$  S.E. of mRNA measurements from 29 small and 21 large DRG neurons.

To investigate the relationship between  $\text{Na}_v1.7$  and  $\beta$  subunits, the mRNAs encoding these subunits were quantitatively measured in small and large DRG neurons. Fig. 2 plots the number of  $\text{Na}_v1.7$  mRNA copies versus the  $\beta$  subunit mRNA measured from the same neurons. The data were statistically evaluated using Pearson product-moment correlation analysis to determine the strength of mRNA coexpression in these neurons. The  $\text{Na}_v1.7$ - $\beta_2$  and  $\text{Na}_v1.7$ - $\beta_3$  mRNAs were found to be significantly correlated, with Pearson coefficients ( $r$ ) of 0.777 and 0.775, respectively ( $p < 0.001$ ). Despite the low expression of  $\beta_1$  mRNA (344 copies/neurons), these subunits were significantly correlated with  $\text{Na}_v1.7$  ( $r = 0.537$ ,  $p < 0.01$ ), although the physiological relevance of this association is not clear. The  $\text{Na}_v1.7$  and  $\beta_4$  mRNAs were not associated in these neurons ( $r = 0.193$ ). These data indicate that  $\beta_2$  and  $\beta_3$  subunit transcripts are abundantly expressed in small DRG neurons and are significantly correlated with  $\text{Na}_v1.7$  mRNA.

Fig. 2 also shows the correlation of  $\text{Na}_v1.7$  and  $\beta$  subunit mRNAs in large neurons.  $\text{Na}_v1.7$  expression was significantly correlated with the  $\beta_1$  ( $r = 0.732$ ) and  $\beta_2$  ( $r = 0.680$ ) subunits ( $p < 0.001$ ). This contrasted with the  $\beta_3$  ( $r = 0.357$ ,  $p = 0.112$ ) and  $\beta_4$  ( $r = 0.342$ ,  $p = 0.152$ ) subunits, which were not correlated with  $\text{Na}_v1.7$ . The data indicate that the  $\text{Na}_v1.7$ ,  $\beta_1$  subunit, and  $\beta_2$  subunit mRNAs are coexpressed in the same population of large-diameter neurons.

$\text{Na}_v1.7$ - $\beta$  interactions were further investigated using co-immunoprecipitation and Western blotting (Fig. 3). Fig. 3A shows a Western blot of DRG homogenates isolated from postnatal day 7 animals probed with the anti- $\text{Na}_v1.7$  antibody. The anti- $\text{Na}_v1.7$  antibody labeled a single high molecular mass protein

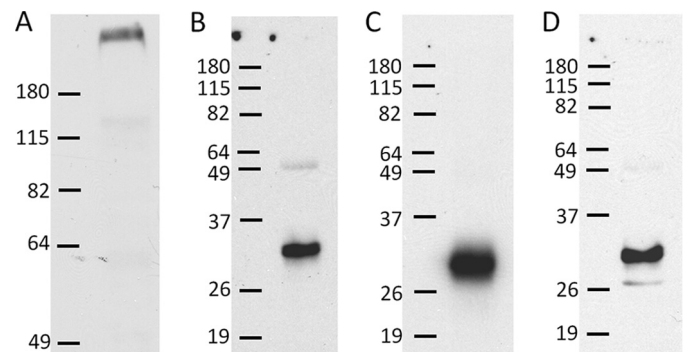


**FIGURE 3. Co-immunoprecipitation of  $\text{Na}_v1.7$  and  $\beta$  subunits.** DRG homogenates were separated on SDS-polyacrylamide gels, transferred to nitrocellulose membranes, and probed with  $\text{Na}_v1.7$ -specific antibodies (A).  $\text{Na}_v1.7$  channel complexes were immunoprecipitated from DRG lysates; separated on SDS-polyacrylamide gels; and probed with antibodies specific for  $\beta_1$  (B),  $\beta_2$  (C), and  $\beta_3$  (D). Bars indicate the positions of molecular mass markers (shown in kilodaltons).

( $\approx 270$  kDa) that is characteristic of  $\text{Na}_v1.7$  channels. Immunoprecipitated  $\text{Na}_v1.7$  complexes were separated on acrylamide gels, transferred to nitrocellulose membranes, and probed with  $\beta$ -specific antibodies. Fig. 3 (B–D) shows that the anti- $\beta$  subunit antibodies labeled low molecular mass proteins (32–34 kDa) that are slightly smaller than what was previously reported for the  $\beta_1$  (36 kDa) and  $\beta_2$  (33 kDa) subunits of adult rats (24).  $\beta$  subunits are highly glycosylated proteins containing 30–36% carbohydrate by weight (24, 25). Differences in the carbohydrate content of these subunits account for variations in the molecular mass of the  $\beta_1$  subunit expressed in skeletal muscle (25). We speculate that the lower molecular masses observed in P7 animals ( $\approx 1$ –2 kDa) may represent partially glycosylated  $\beta$

## Differential Expression of $\beta$ Subunits in DRG Neurons

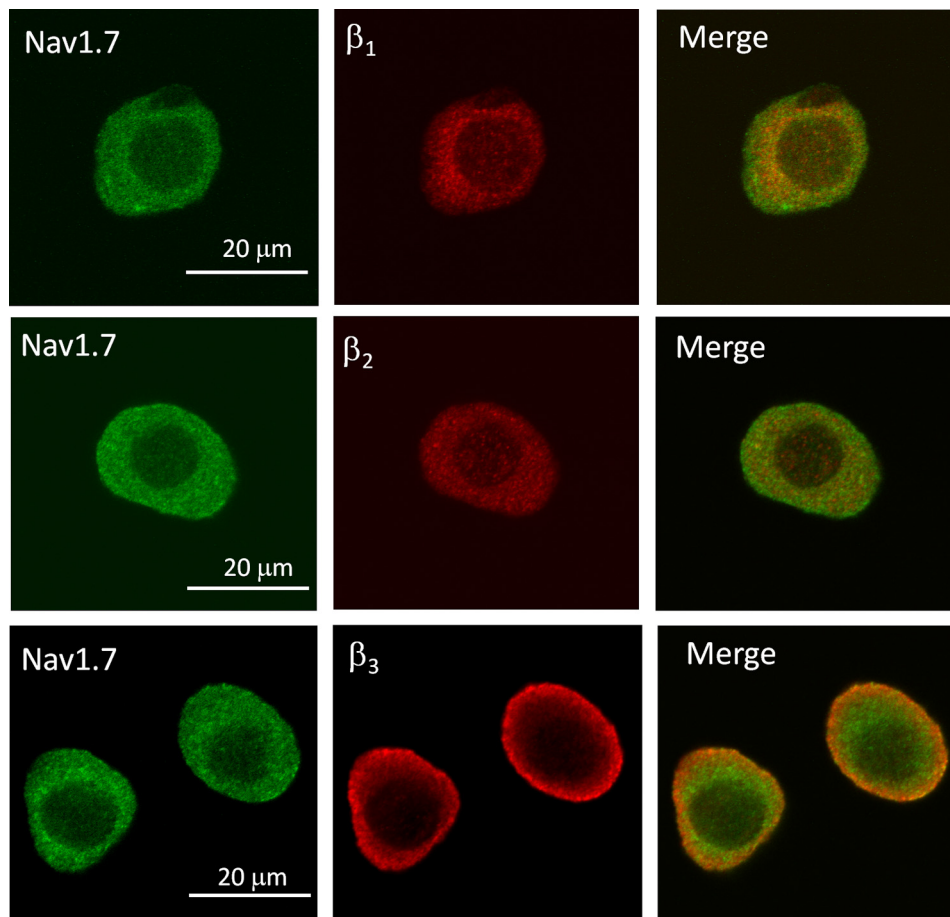


FIGURE 4. **Imaging of  $\text{Na}_v1.7$  and  $\beta$  subunits in small DRG neurons.** Small-diameter DRG neurons ( $<25 \mu\text{m}$ ) were immunolabeled with  $\text{Na}_v1.7$ - and  $\beta$ -specific ( $\beta_1$ – $\beta_3$ ) antibodies and reacted with fluorochrome-conjugated secondary antibodies before confocal imaging. *Left panels*,  $\text{Na}_v1.7$  immunostaining; *middle panels*,  $\beta$  subunit staining; *right panels*, merged images.

subunits (26). The immunoprecipitation data show that the  $\beta_1$ – $\beta_3$  subunits formed stable complexes with  $\text{Na}_v1.7$  channels isolated from the DRG and are therefore candidates for regulating these channels *in vivo*. Unfortunately, it is impossible to associate the  $\text{Na}_v1.7$ – $\beta$  interactions detected using immunoblotting techniques with specific subpopulations of small and large DRG neurons.

Potential  $\text{Na}_v1.7$ – $\beta$  subunit interactions were further investigated by immunocytochemistry. Fig. 4 shows the confocal imaging of small neurons labeled with  $\text{Na}_v1.7$ - and  $\beta$ -specific antibodies. The cytoplasm of these neurons displayed diffuse labeling for  $\text{Na}_v1.7$  and the  $\beta_1$  and  $\beta_2$  subunits. Merged images revealed some overlap of  $\text{Na}_v1.7$  with the  $\beta_1$  and  $\beta_2$  subunits, predominately within the intracellular compartment. By contrast, the majority of the  $\beta_3$  immunofluorescence was localized along the cell periphery, consistent with the labeling of membrane-bound proteins. The merged images display considerable overlap of  $\text{Na}_v1.7$  and  $\beta_3$  around the cell periphery, consistent with the co-localization of these proteins near the plasma membrane.

Initial attempts to investigate the  $\beta$  subunit regulation of endogenous  $\text{Na}_v1.7$  channels in dissociated DRG neurons were complicated by the variable expression of  $\text{Na}_v1.7$  and  $\beta$  subunits and the presence of multiple overlapping components of TTX-S  $\text{Na}^+$  current in these neurons. We therefore conducted

heterologous expression studies to further investigate the  $\beta$  subunit regulation of  $\text{Na}_v1.7$  channels. HEK293 cells stably expressing  $\text{Na}_v1.7$  were transiently transfected with  $\beta$  subunits. Fig. 5 shows examples of whole-cell  $\text{Na}^+$  currents recorded from cells expressing  $\text{Na}_v1.7$  alone or with coexpressed  $\beta_1$  or  $\beta_3$  subunits. In the absence of  $\beta$  subunits, the  $\text{Na}_v1.7$  channels produced rapidly gating  $\text{Na}^+$  current. Coexpressing  $\beta$  subunits ( $\beta_1$ – $\beta_4$ ) had no effect on the current kinetics or peak  $\text{Na}^+$  current amplitudes.

To investigate potential changes in voltage-dependent gating, the  $\text{Na}^+$  conductance was calculated from the peak currents and plotted *versus* the test voltage (Fig. 6A). Coexpressing the  $\beta_3$  subunit produced a significant hyperpolarizing shift ( $-9 \text{ mV}$ ) in  $\text{Na}_v1.7$  activation. Steady-state inactivation was determined using 500-ms prepulses to voltages between  $-130$  and  $-5 \text{ mV}$ .  $\beta_1$  induced a depolarizing shift ( $+5 \text{ mV}$ ) in the midpoint of  $\text{Na}_v1.7$  inactivation (Fig. 6A). By contrast, coexpressing the  $\beta_2$  or  $\beta_4$  subunits did not alter the activation or the steady-state inactivation of the channels.

Recovery from inactivation was determined by applying depolarizing prepulses ( $-20 \text{ mV}/30 \text{ ms}$ ) before returning to  $-100 \text{ mV}$  for varying intervals ( $0$ – $1200 \text{ ms}$ ). The recovery time course of  $\text{Na}_v1.7$  channels was biexponential, with  $\tau_f$  and  $\tau_s$  time constants of 26 and 153 ms, respectively (Fig. 6B). Coexpressing  $\beta_1$  significantly reduced both  $\tau_f$  (14 ms) and  $\tau_s$  (67 ms), consis-

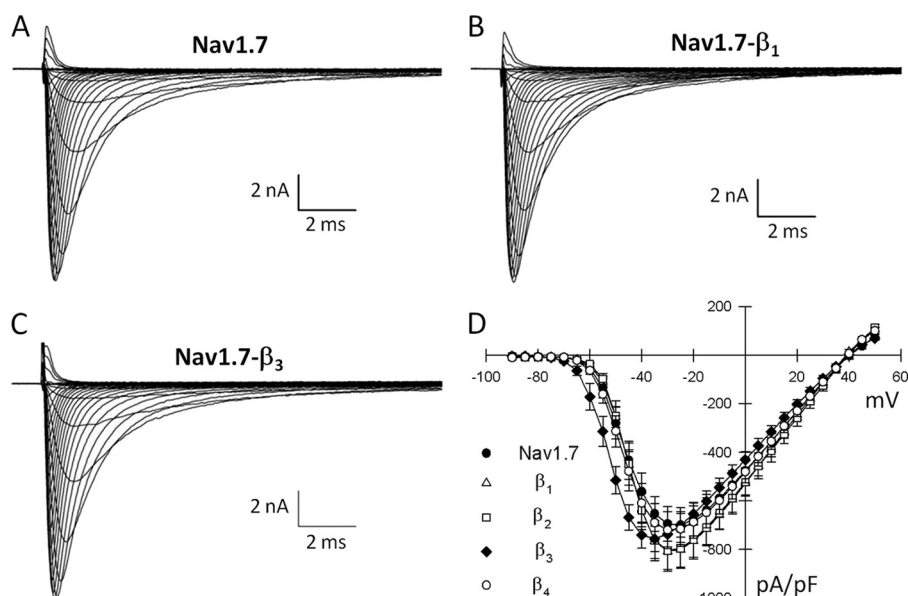


FIGURE 5.  $\beta$  subunit regulation of heterologously expressed  $\text{Na}_v1.7$  channels. Shown are whole-cell  $\text{Na}^+$  currents of HEK293 cells stably expressing the  $\text{Na}_v1.7$  channels. Currents were elicited by depolarizing voltage pulses between  $-90$  and  $+50$  mV from a holding potential of  $-120$  mV. A–C, representative  $\text{Na}^+$  currents of  $\text{Na}_v1.7$  channels expressed alone (A) or coexpressed with  $\beta_1$  (B) or  $\beta_3$  (C) subunits. D, plot of the peak current density (picoamperes/picofarads) of  $\text{Na}_v1.7$  channels alone or coexpressed with  $\beta$  subunits ( $\beta_1$ – $\beta_4$ ). Data are the means  $\pm$  S.E. of 13 ( $\text{Na}_v1.7$ ), 26 ( $\beta_1$ ), 9 ( $\beta_2$ ), 18 ( $\beta_3$ ), and 8 ( $\beta_4$ ) determinations.

tent with a more rapid recovery from inactivation (Fig. 6B). The remaining  $\beta$  subunits ( $\beta_2$ – $\beta_4$ ) had no effect on recovery from inactivation (Table 1).

The overlap of activation and steady-state inactivation of  $\text{Na}^+$  channels defines a range of voltages (*i.e.* window) where  $\text{Na}^+$  channels can be partially activated but are not fully inactivated.  $\text{Na}^+$  channels within this hyperpolarized range of voltages may become persistently activated, resulting in inward  $\text{Na}^+$  currents that could potentially depolarize the resting membrane potential and increase neuronal excitability.  $\beta$  subunit-induced increases in the overlap of  $\text{Na}^+$  channel activation and inactivation tend to expand this window and, consequently, the fraction of persistently activated channels. The  $\beta_1$  subunit produced a  $+5$ -mV depolarizing shift in steady-state inactivation, whereas  $\beta_3$  produced a  $-9$ -mV shift in  $\text{Na}_v1.7$  activation (Table 1) that could potentially increase the window currents. Fig. 6C shows the predicted window currents of  $\text{Na}_v1.7$  channels coexpressed with either the  $\beta_1$  or  $\beta_3$  subunits. Despite acting by different mechanisms, the  $\beta_1$  and  $\beta_3$  subunits produced similar 2–3-fold increases in the  $\text{Na}_v1.7$  window current.

To gain a better understanding of the mechanism of  $\beta$  subunit regulation, chimeras were generated by exchanging the structural domains of the  $\beta_1$  subunit that shifted steady-state inactivation and accelerated recovery from inactivation with the homologous domains of the  $\beta_2$  subunit that had no effect on  $\text{Na}_v1.7$  gating (Table 1). The extracellular N-terminal, intracellular C-terminal, and membrane-spanning domains of  $\beta_1$  were systematically replaced with those of  $\beta_2$  and transiently expressed in HEK293 cells stably expressing  $\text{Na}_v1.7$  channels. Chimeras that retained the extracellular N-terminal domain of  $\beta_1$  ( $\beta_{112}$  and  $\beta_{11\Delta}$ ) fully recapitulated the hyperpolarizing shift in steady-state inactivation and faster recovery observed with the wild-type  $\beta_1$  subunit (Table 1). Conversely, substitutions that replaced the N terminus of  $\beta_1$  ( $\beta_{211}$  and  $\beta_{221}$ ) completely

abolished  $\text{Na}_v1.7$  regulation. C-terminal deletions of the  $\beta_1$  subunit ( $\beta_{11\Delta}$ ) retained full activity, indicating that the intracellular domain is not essential. The data indicate that the extracellular N-terminal domain of  $\beta_1$  is critical for the functional regulation of  $\text{Na}_v1.7$  channels.

## DISCUSSION

The goal of this study was to investigate the expression of auxiliary  $\beta$  subunits in DRG neurons and to characterize the  $\beta$  subunit regulation of  $\text{Na}_v1.7$ , a TTX-S  $\text{Na}^+$  channel widely expressed in sensory neurons. Single-cell analysis demonstrated that  $\beta$  subunit mRNAs were differentially expressed in small ( $\beta_2$  and  $\beta_3$ ) and large ( $\beta_1$  and  $\beta_2$ ) DRG neurons (Fig. 1). Comparisons of  $\text{Na}_v1.7$ ,  $\beta_2$ , and  $\beta_3$  mRNAs measured in individual small neurons showed that the expression of these subunits was significantly correlated (Fig. 2), indicating that these transcripts are coexpressed in the same neurons. By contrast, the  $\text{Na}_v1.7$  mRNA of large neurons was found to be significantly correlated with the  $\beta_1$  and  $\beta_2$  subunits. These data indicate that the  $\text{Na}_v1.7$  channels present in small and large DRG neurons are coexpressed with different complements of auxiliary  $\beta$  subunits.

Interactions between  $\text{Na}_v1.7$  and  $\beta$  subunits were further explored by co-immunoprecipitation of  $\text{Na}_v1.7$  channels.  $\text{Na}_v1.7$  coprecipitated with the  $\beta_1$ – $\beta_3$  subunits (Fig. 3), indicating that these subunits form stable complexes *in vivo*. Despite supporting a direct physical interaction between  $\text{Na}_v1.7$  and the  $\beta_1$ – $\beta_3$  subunits, it is impossible to ascertain the neurons in which these interactions occurred (*i.e.* small *versus* large) using immunoprecipitation techniques. However, immunofluorescence imaging showed that  $\text{Na}_v1.7$  and  $\beta_3$  co-localized near the periphery of the small DRG neurons (Fig. 4). Although  $\beta_2$  subunits are also highly expressed in small neurons, they failed to display obvious co-localization with  $\text{Na}_v1.7$  channels. The combination of  $\text{Na}_v1.7$ – $\beta_3$  mRNA correlation (Fig. 2), co-immuno-



## Differential Expression of $\beta$ Subunits in DRG Neurons

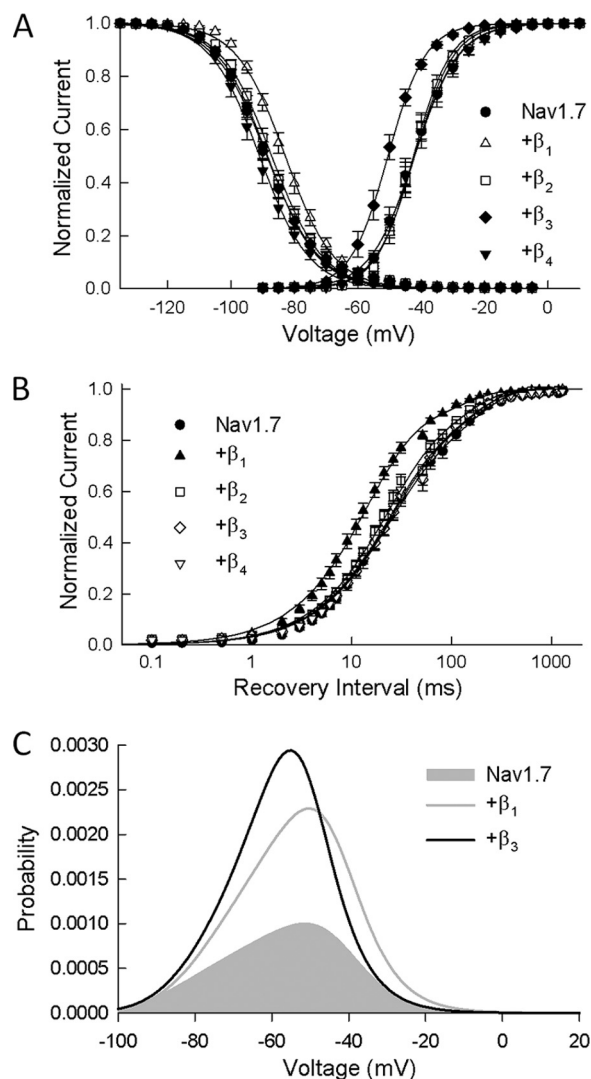


**FIGURE 6.  $\beta$  subunits shift activation and inactivation of  $\text{Na}_v1.7$  channels.** A, the normalized conductance was determined from the peak  $\text{Na}^+$  currents and is plotted versus the test potential. Also plotted is the steady-state inactivation obtained using 500-ms prepulses to voltages between  $-130$  and  $-5$  mV. The smooth curves are fits of the activation and inactivation data to Boltzmann functions with the parameters listed in Table 1. Data are the means  $\pm$  S.E. of 14 ( $\text{Na}_v1.7$ ), 26 ( $\beta_1$ ), 9 ( $\beta_2$ ), 21 ( $\beta_3$ ), and 8 ( $\beta_4$ ) determinations. B,  $\text{Na}^+$  channels were inactivated by a brief depolarization ( $-30$  mV/20 ms), and the recovery time course (0–1200 ms) was measured at  $-100$  mV. The smooth curves are biexponential curve fits with the fast and slow time constants listed in Table 1. Data are the means  $\pm$  S.E. of 15 ( $\text{Na}_v1.7$ ), 22 ( $\beta_1$ ), 10 ( $\beta_2$ ), 17 ( $\beta_3$ ), and 8 ( $\beta_4$ ) determinations. C, window current probabilities predicted from the activation and steady-state inactivation of the  $\text{Na}_v1.7$  channels expressed alone or with either the  $\beta_1$  or  $\beta_3$  subunits.

precipitation (Fig. 3), and co-localization near the plasma membrane (Fig. 4) supports the idea that  $\beta_3$  subunits partner with  $\text{Na}_v1.7$  channels. Although these data do not preclude  $\text{Na}_v1.7$  interaction with other  $\beta$  subunits, they suggest an important contribution of  $\text{Na}_v1.7$ - $\beta_3$  channels to the TTX-S  $\text{Na}^+$  currents of small DRG neurons.

Previous studies of  $\beta$  subunit regulation of heterologously expressed  $\text{Na}_v1.7$  channels have produced conflicting data. Initial studies of  $\text{Na}_v1.7$  channels expressed in *Xenopus* oocytes indicated that the  $\beta_1$  and  $\beta_2$  subunits failed to alter the expression or gating properties of  $\text{Na}_v1.7$ , suggesting that these channels may be not regulated by these auxiliary subunits (27, 28).

Subsequent work, also in oocytes, found that coexpressing  $\beta_1$  accelerated inactivation and recovery kinetics and produced a hyperpolarizing shift in  $\text{Na}_v1.7$  activation (29). The regulation of  $\text{Na}_v1.7$  channels by the  $\beta_3$  and  $\beta_4$  subunits has not been investigated.

In this study, HEK293 cells stably expressing  $\text{Na}_v1.7$  channels were employed to further investigate the functional consequences of  $\text{Na}_v1.7$ - $\beta$  interactions. Coexpressing  $\beta$  subunits ( $\beta_1$ – $\beta_4$ ) did not alter the peak  $\text{Na}^+$  current densities or  $\text{Na}_v1.7$  current kinetics. However,  $\beta_1$  produced a depolarizing shift in steady-state inactivation and a faster recovery from inactivation (Table 1). At voltages near the resting membrane potentials of DRG neurons ( $\approx -60$  mV), depolarizing shifts in inactivation would tend to increase the fraction of  $\text{Na}_v1.7$  channels available to open in response to depolarization. Similar increases in availability along with the associated increase in  $\text{Na}^+$  current density are well known to reduce the threshold for initiating action potentials (30–32). The rate of  $\text{Na}^+$  channel recovery from inactivation is an important determinant of the absolute and relative refractory periods of action potentials. The faster recovery of  $\text{Na}_v1.7$ - $\beta_1$  channels predicts rapid repriming at hyperpolarized voltages that may reduce the duration of the refractory periods, thereby enabling increased firing frequency in large-diameter neurons highly expressing the  $\text{Na}_v1.7$ - $\beta_1$  combination.

The  $\beta_3$  subunit produced a  $-9$ -mV shift in  $\text{Na}_v1.7$  activation, causing the channels to open at more hyperpolarized voltages (Table 1). Such shifts in activation and the accompanying increase in  $\text{Na}^+$  current at more hyperpolarized voltages are predicted to increase neuronal excitability and could potentially reduce the threshold for firing action potentials in small-diameter neurons. This mechanism is consistent with studies showing that  $\text{Na}^+$  channels with low activation thresholds are critical determinants of action potential initiation at the axon initial segment (33, 34).

$\text{Na}_v1.7$ - $\beta$  subunit interactions that induce hyperpolarizing shifts in activation ( $\beta_3$ ) or depolarizing shifts in inactivation ( $\beta_1$ ) tend to increase the overlap of activation and inactivation gating (Fig. 6C). At voltages within this overlap region,  $\text{Na}^+$  channels are partially activated but not fully inactivated, increasing the potential of persistent window currents (35). At  $-50$  mV, the peak window current probability predicts that a small percentage (0.1%) of  $\text{Na}_v1.7$  channels will be persistently activated. Coexpressing the  $\beta_1$  or  $\beta_3$  subunits increased the probability of persistent activation by 2–3-fold. Persistent activation of  $\text{Na}_v1.7$ - $\beta_1$  and  $\text{Na}_v1.7$ - $\beta_3$  channels and the resulting inward  $\text{Na}^+$  current at resting membrane potentials could depolarize the neuron, leading to increased excitability of DRG neurons. Similar mechanisms are believed to underlie the increased excitability of sensory neurons harboring inherited human pain disorder mutations that produce shifts in  $\text{Na}_v1.7$  activation and inactivation of similar polarity and magnitude as those observed for the  $\text{Na}_v1.7$ - $\beta_1$  and  $\text{Na}_v1.7$ - $\beta_3$  channels (36–38).

Previous studies have employed chimeras, deletion analysis, and mutations to define the structural domains of  $\beta$  subunits that are critical for  $\text{Na}^+$  channel regulation (21, 39–42). The findings indicate that the extracellular N-terminal domain of  $\beta_1$

TABLE 1

 $\beta$  subunit regulation of Nav1.7 gating

The parameters were obtained from curve fits of  $\text{Na}_v1.7$  activation, inactivation, and recovery from inactivation (Fig. 6). The data were tested for significant differences by analysis of variance ( $p < 0.001$ ), followed by Dunnett's post hoc test at a significance level of  $p < 0.05$ . For Dunnett's test, the effects of  $\beta$  subunits were compared with values measured for  $\text{Na}_v1.7$  channels expressed alone. Data are the means  $\pm$  S.E. of between 8 and 30 experiments.

	Activation		Inactivation		Recovery		
	$V_{0.5}$	$k_v$	$V_{0.5}$	$k_v$	$\tau_f$	$\tau_s$	$A_f$
$\text{Na}_v1.7$	$-42 \pm 1$	$6.0 \pm 0.3$	$-88 \pm 2$	$7.2 \pm 0.3$	$26 \pm 2$	$153 \pm 11$	68
$\beta_1$	$-43 \pm 1$	$5.7 \pm 0.3$	$-83 \pm 1^a$	$7.2 \pm 0.2$	$14 \pm 1^a$	$67 \pm 7^a$	67
$\beta_2$	$-43 \pm 1$	$5.3 \pm 0.3$	$-87 \pm 1$	$7.2 \pm 0.2$	$22 \pm 2$	$128 \pm 12$	70
$\beta_3$	$-51 \pm 1^a$	$5.0 \pm 0.3$	$-88 \pm 1$	$7.1 \pm 0.2$	$24 \pm 2$	$142 \pm 11$	70
$\beta_4$	$-41 \pm 1$	$6.9 \pm 0.2$	$-91 \pm 2$	$7.6 \pm 1.0$	$25 \pm 2$	$136 \pm 11$	73
<b><math>\beta_1/\beta_2</math> chimeras</b>							
$\beta_{112}$	$-44 \pm 1$	$5.9 \pm 0.2$	$-83 \pm 1^a$	$6.3 \pm 0.1$	$16 \pm 1^a$	$58 \pm 6^a$	73
$\beta_{11\Delta}$	$-44 \pm 1$	$4.9 \pm 0.2$	$-82 \pm 1^a$	$6.3 \pm 0.2$	$16 \pm 2^a$	$60 \pm 6^a$	71
$\beta_{211}$	$-43 \pm 1$	$5.4 \pm 0.3$	$-87 \pm 1$	$7.2 \pm 0.2$	$22 \pm 1$	$126 \pm 11$	69
$\beta_{221}$	$-44 \pm 1$	$4.6 \pm 0.2$	$-88 \pm 1$	$6.9 \pm 0.2$	$22 \pm 2$	$133 \pm 10$	67

<sup>a</sup> Values indicate significant differences ( $p < 0.05$ ).

is essential for the functional regulation of neuronal and skeletal muscle  $\text{Na}^+$  channels. This contrasts with the  $\beta_1$  regulation of cardiac  $\text{Na}^+$  channels, where the membrane-spanning domain was found to be critical for the increased expression and accelerated recovery of  $\text{Na}_v1.5$  channels (43). These data imply that different structural domains and therefore different molecular interactions are responsible for  $\beta_1$  regulation of neuronal and cardiac  $\text{Na}^+$  channels.

$\beta_1$  mRNA is highly expressed in large DRG neurons (Fig. 1), where it is significantly correlated with  $\text{Na}_v1.7$ , indicating that these subunits are coexpressed in the same population of large-diameter neurons (Fig. 2).  $\beta$  subunit chimeras were employed to identify the structural domains of  $\beta_1$  required to produce the observed depolarizing shift in steady-state inactivation and the accelerated recovery of  $\text{Na}_v1.7$  channels (Table 1). Chimeras incorporating the extracellular N-terminal domain of  $\beta_1$  ( $\beta_{112}$ ) retained the shift in inactivation and faster recovery, whereas replacing the extracellular domain ( $\beta_{211}$ ) completely eliminated these effects. These data indicate that the N-terminal domain of the  $\beta_1$  subunit is required for  $\text{Na}_v1.7$  regulation.  $\beta_1$  subunits with a truncated C terminus ( $\beta_{11\Delta}$ ) retained full functional regulation, indicating that the intracellular domain is nonessential. Interactions between the N terminus of  $\beta_1$  and extracellular loops of  $\text{Na}_v1.7$  may be important for the functional regulation of these channels, similar to what has been described previously for other neuronal  $\text{Na}^+$  channels (40, 41).

Recent work employed a similar approach to investigate the  $\beta_1$  regulation of  $\text{Na}_v1.8$ , a TTX-R channel that produces the majority of the inward  $\text{Na}^+$  current in small-diameter DRG neurons (21). Substitution of the extracellular N-terminal domain of  $\beta_1$  had no effect on the expression or gating properties of  $\text{Na}_v1.8$  channels. Rather, the intracellular C-terminal domain of  $\beta_1$  was found to be the critical determinant of  $\text{Na}_v1.8$  regulation. These data indicate that the N and C termini of the  $\beta_1$  subunit differentially regulate the gating properties of  $\text{Na}_v1.7$  and  $\text{Na}_v1.8$  channels.

Much of what is currently known about  $\beta$  subunit expression in the DRG has been derived from immunocytochemistry and *in situ* hybridization (4, 12, 15–18, 44). These studies indicate that all four isoforms of  $\beta$  subunits ( $\beta_1$ – $\beta_4$ ) are present in the DRG and that these subunits are differentially expressed in subpopulations of sensory neurons (12, 15).  $\beta_3$  subunits are prom-

inently expressed in small and medium neurons, whereas  $\beta_1$  and  $\beta_4$  are preferentially expressed in large neurons (4, 16, 17).  $\beta_2$  appears to be widely expressed in the DRG and does not show a clear preference for neuronal size (15, 45). These findings are in good agreement with our single-cell analysis of gene expression and are consistent with the conclusion that  $\beta$  subunits are differentially expressed in subpopulations of DRG neurons. Unfortunately, histological approaches do not provide quantitative assessments of  $\beta$  subunit expression levels or insight into the functional regulation of  $\text{Na}^+$  channels by  $\beta$  subunits. Our data indicate that the differential expression of  $\beta$  subunits in DRG neurons combined with isoform-specific  $\beta$  subunit regulation of  $\text{Na}_v1.7$  activation ( $\beta_3$ ) and inactivation ( $\beta_1$ ) predicts substantial differences in the predominant TTX-S  $\text{Na}^+$  currents of small and large sensory neurons.

Previous work investigated the role of the  $\beta_1$  and  $\beta_2$  subunits in sensory neurons using *Scn1b* and *Scn2b* null mice (45, 46). Whole-cell recordings from DRG neurons isolated from the  $\beta_1$  knock-outs revealed small changes in the amplitudes and gating properties of TTX-S and TTX-R  $\text{Na}^+$  currents (46). The relatively subtle effects of the *Scn1b* knock-out on DRG  $\text{Na}^+$  currents coupled with the low level expression of  $\beta_1$  subunits in small-diameter sensory neurons suggest that these subunits may not be important regulators of the  $\text{Na}^+$  channels expressed in nociceptors. Neurons from the *Scn2b* null mice displayed reductions in TTX-S  $\text{Na}^+$  current amplitude and  $\text{Na}^+$  channel mRNA and protein (46). Although the underlying mechanism is unclear, the *Scn2b* knock-out appears to reduce TTX-S  $\text{Na}^+$  currents by decreasing  $\text{Na}^+$  channel mRNA and protein expression. Based on the comparison of  $\text{Na}^+$  currents recorded from control and *Scn2b* null mice, the  $\beta_2$  subunits were proposed to increase  $\text{Na}^+$  channel expression ( $\text{Na}_v1.1$ ,  $\text{Na}_v1.6$ , and  $\text{Na}_v1.7$ ), produce hyperpolarizing shifts in activation, and accelerate the kinetics of the endogenous TTX-S  $\text{Na}^+$  currents (46). These effects were not recapitulated in our heterologous expression studies of  $\text{Na}_v1.7$ - $\beta_2$  channels, where no changes in  $\text{Na}^+$  current density, voltage dependence, or current kinetics were observed. Rather, our findings are consistent with previous work showing that the  $\beta_2$  subunit has no effect on the expression or gating properties of the  $\text{Na}_v1.3$ ,  $\text{Na}_v1.6$ , and  $\text{Na}_v1.8$  channels (21, 47). The reasons for the apparent discrepancy between *in vivo* knockdown and heterologous expression



## Differential Expression of $\beta$ Subunits in DRG Neurons

studies are not known but may reflect contributions by endogenous regulatory pathways that are specific to the DRG or the compensatory up-regulation of other  $\beta$  subunits in the sensory neurons of *Scn2b* null mice.

### REFERENCES

- Cummins, T. R., Sheets, P. L., and Waxman, S. G. (2007) The roles of sodium channels in nociception: implications for mechanisms of pain. *Pain* **131**, 243–257
- Dib-Hajj, S. D., Binshtok, A. M., Cummins, T. R., Jarvis, M. F., Samad, T., and Zimmermann, K. (2009) Voltage-gated sodium channels in pain states: role in pathophysiology and targets for treatment. *Brain Res. Rev.* **60**, 65–83
- Rush, A. M., Cummins, T. R., and Waxman, S. G. (2007) Multiple sodium channels and their roles in electrogenesis within dorsal root ganglion neurons. *J. Physiol.* **579**, 1–14
- Black, J. A., Dib-Hajj, S., McNabola, K., Jeste, S., Rizzo, M. A., Kocsis, J. D., and Waxman, S. G. (1996) Spinal sensory neurons express multiple sodium channel  $\alpha$  subunit mRNAs. *Brain Res. Mol. Brain Res.* **43**, 117–131
- Dib-Hajj, S. D., Tyrrell, L., Black, J. A., and Waxman, S. G. (1998) Na<sub>v</sub>1, a novel voltage-gated sodium channel, is expressed preferentially in peripheral sensory neurons and down-regulated after axotomy. *Proc. Natl. Acad. Sci. U.S.A.* **95**, 8963–8968
- Amaya, F., Decosterd, I., Samad, T. A., Plumpton, C., Tate, S., Mannion, R. J., Costigan, M., and Woolf, C. J. (2000) Diversity of expression of the sensory neuron-specific TTX-resistant voltage-gated sodium ion channels SNS and SNS2. *Mol. Cell. Neurosci.* **15**, 331–342
- Ho, C., and O'Leary, M. E. (2011) Single-cell analysis of sodium channel expression in dorsal root ganglion neurons. *Mol. Cell. Neurosci.* **46**, 159–166
- Isom, L. L., Scheuer, T., Brownstein, A. B., Ragsdale, D. S., Murphy, B. J., and Catterall, W. A. (1995) Functional coexpression of the  $\beta_1$  and type IIA  $\alpha$  subunits of sodium channels in a mammalian cell line. *J. Biol. Chem.* **270**, 3306–3312
- Catterall, W. A. (2000) From ionic currents to molecular mechanisms: the structure and function of voltage-gated sodium channels. *Neuron* **26**, 13–25
- Isom, L. L. (2001) Sodium channel  $\beta$  subunits: anything but auxiliary. *Neuroscientist* **7**, 42–54
- Isom, L. L. (2002) The role of sodium channels in cell adhesion. *Front. Biosci.* **7**, 12–23
- Coward, K., Jowett, A., Plumpton, C., Powell, A., Birch, R., Tate, S., Bountra, C., and Anand, P. (2001) Sodium channel  $\beta_1$  and  $\beta_2$  subunits parallel SNS/PN3  $\alpha$  subunit changes in injured human sensory neurons. *Neuroreport* **12**, 483–488
- Isom, L. L., De Jongh, K. S., Patton, D. E., Reber, B. F., Offord, J., Charbonneau, H., Walsh, K., Goldin, A. L., and Catterall, W. A. (1992) Primary structure and functional expression of the  $\beta_1$  subunit of the rat brain sodium channel. *Science* **256**, 839–842
- Morgan, K., Stevens, E. B., Shah, B., Cox, P. J., Dixon, A. K., Lee, K., Pinnock, R. D., Hughes, J., Richardson, P. J., Mizuguchi, K., and Jackson, A. P. (2000)  $\beta_3$ : an additional auxiliary subunit of the voltage-sensitive sodium channel that modulates channel gating with distinct kinetics. *Proc. Natl. Acad. Sci. U.S.A.* **97**, 2308–2313
- Takahashi, N., Kikuchi, S., Dai, Y., Kobayashi, K., Fukuoka, T., and Noguchi, K. (2003) Expression of auxiliary  $\beta$  subunits of sodium channels in primary afferent neurons and the effect of nerve injury. *Neuroscience* **121**, 441–450
- Oh, Y., Sashihara, S., Black, J. A., and Waxman, S. G. (1995) Na<sup>+</sup> channel  $\beta_1$  subunit mRNA: differential expression in rat spinal sensory neurons. *Brain Res. Mol. Brain Res.* **30**, 357–361
- Shah, B. S., Stevens, E. B., Gonzalez, M. I., Bramwell, S., Pinnock, R. D., Lee, K., and Dixon, A. K. (2000)  $\beta_3$ , a novel auxiliary subunit for the voltage-gated sodium channel, is expressed preferentially in sensory neurons and is up-regulated in the chronic constriction injury model of neuropathic pain. *Eur. J. Neurosci.* **12**, 3985–3990
- Yu, F. H., Westenbroek, R. E., Silos-Santiago, I., McCormick, K. A., Lawson, D., Ge, P., Ferriera, H., Lilly, J., DiStefano, P. S., Catterall, W. A., Scheuer, T., and Curtis, R. (2003) Sodium channel  $\beta_3$ , a new disulfide-linked auxiliary subunit with similarity to  $\beta_2$ . *J. Neurosci.* **23**, 7577–7585
- Lampert, A., O'Reilly, A. O., Reeh, P., and Leffler, A. (2010) Sodium channelopathies and pain. *Pflugers Arch.* **460**, 249–263
- Fischer, T. Z., and Waxman, S. G. (2010) Familial pain syndromes from mutations of the Na<sub>v</sub>1.7 sodium channel. *Ann. N.Y. Acad. Sci.* **1184**, 196–207
- Zhao, J., O'Leary, M. E., and Chahine, M. (2011) Regulation of Na<sub>v</sub>1.6 and Na<sub>v</sub>1.8 peripheral nerve Na<sup>+</sup> channels by auxiliary  $\beta$  subunits. *J. Neurophysiol.* **106**, 608–619
- Vijayaragavan, K., Powell, A. J., Kinghorn, I. J., and Chahine, M. (2004) Role of auxiliary  $\beta_1$ ,  $\beta_2$ , and  $\beta_3$  subunits and their interaction with Na<sub>v</sub>1.8 voltage-gated sodium channel. *Biochem. Biophys. Res. Commun.* **319**, 531–540
- Zhao, J., Ziane, R., Chatelier, A., O'Leary, M. E., and Chahine, M. (2007) Lidocaine promotes the trafficking and functional expression of Na<sub>v</sub>1.8 sodium channels in mammalian cells. *J. Neurophysiol.* **98**, 467–477
- Messner, D. J., and Catterall, W. A. (1985) The sodium channel from rat brain. Separation and characterization of subunits. *J. Biol. Chem.* **260**, 10597–10604
- Roberts, R. H., and Barchi, R. L. (1987) The voltage-sensitive sodium channel from rabbit skeletal muscle. Chemical characterization of subunits. *J. Biol. Chem.* **262**, 2298–2303
- Sutkowski, E. M., and Catterall, W. A. (1990)  $\beta_1$  subunits of sodium channels. Studies with subunit-specific antibodies. *J. Biol. Chem.* **265**, 12393–12399
- Sangameswaran, L., Delgado, S. G., Fish, L. M., Koch, B. D., Jakeman, L. B., Stewart, G. R., Sze, P., Hunter, J. C., Eglén, R. M., and Herman, R. C. (1996) Structure and function of a novel voltage-gated, tetrodotoxin-resistant sodium channel specific to sensory neurons. *J. Biol. Chem.* **271**, 5953–5956
- Sangameswaran, L., Fish, L. M., Koch, B. D., Rabert, D. K., Delgado, S. G., Ilnicka, M., Jakeman, L. B., Novakovic, S., Wong, K., Sze, P., Tzoumakia, E., Stewart, G. R., Herman, R. C., Chan, H., Eglén, R. M., and Hunter, J. C. (1997) A novel tetrodotoxin-sensitive, voltage-gated sodium channel expressed in rat and human dorsal root ganglia. *J. Biol. Chem.* **272**, 14805–14809
- Vijayaragavan, K., O'Leary, M. E., and Chahine, M. (2001) Gating properties of Na<sub>v</sub>1.7 and Na<sub>v</sub>1.8 peripheral nerve sodium channels. *J. Neurosci.* **21**, 7909–7918
- Azouz, R., and Gray, C. M. (2000) Dynamic spike threshold reveals a mechanism for synaptic coincidence detection in cortical neurons *in vivo*. *Proc. Natl. Acad. Sci. U.S.A.* **97**, 8110–8115
- Henze, D. A., and Buzsáki, G. (2001) Action potential threshold of hippocampal pyramidal cells *in vivo* is increased by recent spiking activity. *Neuroscience* **105**, 121–130
- Platkiewicz, J., and Brette, R. (2010) A threshold equation for action potential initiation. *PLoS Comput. Biol.* **6**, e1000850
- Colbert, C. M., and Pan, E. (2002) Ion channel properties underlying axonal action potential initiation in pyramidal neurons. *Nat. Neurosci.* **5**, 533–538
- Hu, W., Tian, C., Li, T., Yang, M., Hou, H., and Shu, Y. (2009) Distinct contributions of Na<sub>v</sub>1.6 and Na<sub>v</sub>1.2 in action potential initiation and back-propagation. *Nat. Neurosci.* **12**, 996–1002
- Attwell, D., Cohen, I., Eisner, D., Ohba, M., and Ojeda, C. (1979) The steady-state TTX-sensitive (“window”) sodium current in cardiac Purkinje fibres. *Pflugers Arch.* **379**, 137–142
- Harty, T. P., Dib-Hajj, S. D., Tyrrell, L., Blackman, R., Hisama, F. M., Rose, J. B., and Waxman, S. G. (2006) Na<sub>v</sub>1.7 mutant A863P in erythromelalgia: effects of altered activation and steady-state inactivation on excitability of nociceptive dorsal root ganglion neurons. *J. Neurosci.* **26**, 12566–12575
- Rush, A. M., Dib-Hajj, S. D., Liu, S., Cummins, T. R., Black, J. A., and Waxman, S. G. (2006) A single sodium channel mutation produces hyper- or hypoexcitability in different types of neurons. *Proc. Natl. Acad. Sci. U.S.A.* **103**, 8245–8250
- Dib-Hajj, S. D., Cummins, T. R., Black, J. A., and Waxman, S. G. (2010)

- Sodium channels in normal and pathological pain. *Annu. Rev. Neurosci.* **33**, 325–347
39. Chen, C., and Cannon, S. C. (1995) Modulation of Na<sup>+</sup> channel inactivation by the  $\beta_1$  subunit: a deletion analysis. *Pflugers Arch.* **431**, 186–195
  40. McCormick, K. A., Isom, L. L., Ragsdale, D., Smith, D., Scheuer, T., and Catterall, W. A. (1998) Molecular determinants of Na<sup>+</sup> channel function in the extracellular domain of the  $\beta_1$  subunit. *J. Biol. Chem.* **273**, 3954–3962
  41. McCormick, K. A., Srinivasan, J., White, K., Scheuer, T., and Catterall, W. A. (1999) The extracellular domain of the  $\beta_1$  subunit is both necessary and sufficient for  $\beta_1$ -like modulation of sodium channel gating. *J. Biol. Chem.* **274**, 32638–32646
  42. Qu, Y., Rogers, J. C., Chen, S. F., McCormick, K. A., Scheuer, T., and Catterall, W. A. (1999) Functional roles of the extracellular segments of the sodium channel  $\alpha$  subunit in voltage-dependent gating and modulation by  $\beta_1$  subunits. *J. Biol. Chem.* **274**, 32647–32654
  43. Zimmer, T., and Benndorf, K. (2002) The human heart and rat brain IIA Na<sup>+</sup> channels interact with different molecular regions of the  $\beta_1$  subunit. *J. Gen. Physiol.* **120**, 887–895
  44. Qu, Y., Curtis, R., Lawson, D., Gilbride, K., Ge, P., DiStefano, P. S., Silos-Santiago, I., Catterall, W. A., and Scheuer, T. (2001) Differential modulation of sodium channel gating and persistent sodium currents by the  $\beta_1$ ,  $\beta_2$ , and  $\beta_3$  subunits. *Mol. Cell. Neurosci.* **18**, 570–580
  45. Lopez-Santiago, L. F., Brackenbury, W. J., Chen, C., and Isom, L. L. (2011) Na<sup>+</sup> channel *Scn1b* gene regulates dorsal root ganglion nociceptor excitability *in vivo*. *J. Biol. Chem.* **286**, 22913–22923
  46. Lopez-Santiago, L. F., Pertin, M., Morisod, X., Chen, C., Hong, S., Wiley, J., Decosterd, I., and Isom, L. L. (2006) Sodium channel  $\beta_2$  subunits regulate tetrodotoxin-sensitive sodium channels in small dorsal root ganglion neurons and modulate the response to pain. *J. Neurosci.* **26**, 7984–7994
  47. Meadows, L. S., Chen, Y. H., Powell, A. J., Clare, J. J., and Ragsdale, D. S. (2002) Functional modulation of human brain Na<sub>v</sub>1.3 sodium channels, expressed in mammalian cells, by auxiliary  $\beta_1$ ,  $\beta_2$ , and  $\beta_3$  subunits. *Neuroscience* **114**, 745–753